Electronic Supplementary Information (ESI)

Modulating carrier transport of Pt-Ag heteronuclear complexes to attain highly efficient OLEDs with narrow-band emission

Zhao-Yi Wang,[acde] Lin-Xi Shi,[ab] Liang-Jin Xu,*[a] Li-Yi Zhang,[a] Jin-Yun Wang,[a] and Zhong-Ning Chen*[ab]

[a] *State Key Laboratory of Structural Chemistry, Fujian Institute of Research on the Structure of Matter, Chinese Academy of Sciences, Fuzhou, Fujian 350002, China.*

[b] *Fujian Science & Technology Innovation Laboratory for Optoelectron Information of China, Fuzhou, Fujian 350108, China.*

[c] *ShanghaiTech University, 393 Middle Huaxia Road, Pudong, Shanghai 201210, China.*

[d] *Shanghai Advanced Research Institute, Chinese Academy of Sciences, 99 Haike Road, Pudong, Shanghai 201210, China.*

[e] *University of Chinese Academy of Sciences, Beijing 100039, China.*

E-mail: xuliangjin@fjirsm.ac.cn; czn@fjirsm.ac.cn

Table S1. Crystallographic Data of the $PtAg_2$ Complexes **1-5**.

	1·$4CH_2Cl_2$	**2**·$4CH_2Cl_2$	**3**·$4CH_2Cl_2$	**4**·$3CHCl_3$·	**5**·$6CH_2Cl_2$
Empirical Formula	$C_{96}H_{100}Ag_2C_{110}O_{12}P_6Pt$	$C_{120}H_{114}Ag_2Cl_8F_6N_2O_6P_6PtS_2$	$C_{104}H_{96}O_{12}P_6C_{110}Ag_2PtS_2$	$C_{107}H_{97}Ag_2Cl_{11}N_4O_{11}P_6$	$C_{126}H_{114}N_6P_6Cl_{12}Ag_2PtO_6S_2F_6$
Formula Weight	2396.90	2738.50	2553.07	2599.46	3008.40
Crystal System	Triclinic	Triclinic	Triclinic	Triclinic	Triclinic
Space Group	*P-1*	*P-1*	*P-1*	*P-1*	*P-1*
a (Å)	12.9220(9)	14.3798(12)	14.2447(10)	15.2948(17)	14.2767(10)
b (Å)	15.4161(10)	15.1217(13)	14.3052(11)	18.341(2)	14.9810(11)
c (Å)	15.5171(11)	15.9141(15)	14.6279(11)	22.261(3)	15.3107(10)
α (deg)	114.362(2)	111.210(3)	107.774(3)	72.206(4)	86.910(3)
β (deg)	92.751(3)	95.400(3)	109.179(2)	73.763(4)	84.744(2)
γ (deg)	113.221(2)	110.171(3)	91.196(2)	72.834(4)	74.999(3)
V ($Å^3$)	2504.5(3)	2932.0(5)	2656.5(3)	5556.7(11)	3148.2(4)
Z	1	1	1	2	1
ρ_{calcd} (g cm^{-3})	1.589	1.551	1.596	1.554	1.587
μ (mm^{-1})	2.201	1.885	2.118	2.014	1.846
Radiation (λ, Å)	0.71073	0.71073	0.71073	0.71073	0.71073
Temperature (K)	100.0	100.0	179.68	149.99	100.04
GOF	1.051	1.071	1.081	1.051	1.035
R1 (F_o) [a]	0.0527	0.0282	0.0360	0.0582	0.0293
wR2 (F_o^2) [b]	0.1366	0.0705	0.0952	0.1453	0.0705

[a] $R1 = \Sigma|F_o-F_c|/\Sigma F_o$, [b] $wR2 = \Sigma[w(F_o^2-F_c^2)^2]/\Sigma[w(F_o)^2)]^{1/2}$

Table S2. The Optimization Procedures of the Devices Based on $PtAg_2$ Complex **4** by Modifying Doping Percentage and Host Materials. [a]

Doping Percentage	Host Materials (ratio)	Lmax (cd m^{-2})	Von (V)	CEmax (cd A^{-1})	PEmax (lm W^{-1})	EQEmax (%)
6%	TCTA : OXD-7 (1 : 1)	4182	3.2	35.2	32.4	9.2
6%	TAPC : OXD-7 (1 : 1)	1939	2.8	25.5	27.2	6.7
6%	mCP : OXD-7 (1 : 1)	11912	4.1	69.5	50.5	18.2
3%	mCP : OXD-7 (1 : 1)	10515	4.2	53.1	30.3	13.9
9%	mCP : OXD-7 (1 : 1)	11360	4.4	57.8	34.5	15.1
6%	mCP : OXD-7 (2 : 1)	9834	4.0	64.3	41.2	16.8
6%	mCP : OXD-7 (1 : 2)	9318	4.7	51.5	28.4	13.5

[a] Device structure: ITO / PEDOT : PSS (40 nm) / Poly-TPD (50 nm) / host materials : $PtAg_2$ (50 nm) / BmPyPb (50 nm) / LiF (1 nm) / Al (100 nm).

Table S3. The Partial Molecular Orbital Compositions (%) by SCPA Approach in the Ground State and the Absorption Transition for Complex **1** in the CH_2Cl_2 Solution Calculated by TD-DFT Method at the PBE1PBE Level.

Orbital	Energy (eV)	MO Contribution (%)			
		Pt (s/p/d)	Ag (s/p/d)	PPP	CCR
L+11	-0.95	3.53 (0/100/0)	10.98 (23/69/8)	72.01	13.47
LUMO	-2.42	16.98 (0/100/0)	20.52 (75/16/9)	51.75	10.75
HOMO	-5.89	16.36 (1/0/99)	1.13 (39/28/33)	3.12	79.39
H-2	-6.68	27.57 (35/0/65)	35.42 (36/12/51)	36.43	0.57

States	E, nm (eV)	O.S.	Transition (Contrib.)	Assignment	Exp. (nm)
S1	448 (2.77)	0.4388	HOMO→LUMO (98%)	^{1}LLCT/^{1}LMCT/^{1}MC	437
S3	362 (3.43)	0.5945	H-2→LUMO (98%)	^{1}MC/^{1}IL/^{1}MLCT	
S25	283 (4.38)	0.2004	HOMO→L+11 (80%)	^{1}LLCT/^{1}MC/^{1}IL	

Table S4. The Partial Molecular Orbital Compositions (%) by SCPA Approach in the Lowest-Energy Triplet State and the Emission Transition for Complex **1** in the CH_2Cl_2 Solution Calculated by TD-DFT Method at the PBE1PBE Level.

Orbital	Energy (eV)	MO Contribution (%)			
		Pt (s/p/d)	Ag (s/p/d)	PPP	CCR
LUMO	-2.62	21.10 (0/100/0)	21.73 (80/10/10)	46.32	10.86
HOMO	-5.70	16.84 (1/0/99)	1.01 (42/35/23)	2.78	79.37
H-1	-6.22	1.41 (0/100/0)	8.42 (46/10/44)	11.83	78.35
H-2	-6.75	27.00 (43/0/57)	35.64 (36/13/50)	36.75	0.61

States	E, nm (eV)	O.S.	Transition (Contrib.)	Assignment	Exp. (nm)
T1	618 (2.00)	0.0000	HOMO→LUMO (90%)	^{3}LLCT/^{3}LMCT/^{3}MC/^{3}IL	563
T2	488 (2.54)	0.0000	H-1→LUMO (72%)	^{3}LLCT/^{3}LMCT/^{3}IL	
T3	416 (2.98)	0.0000	H-2→LUMO (94%)	^{3}MC/^{3}IL/^{3}MLCT	

Table S5. The Partial Molecular Orbital Compositions (%) by SCPA Approach in the Ground State and the Absorption Transition for Complex **2** in the CH_2Cl_2 Solution Calculated by TD-DFT Method at the PBE1PBE Level.

Orbital	Energy (eV)	MO Contribution (%)			
		Pt (s/p/d)	Ag (s/p/d)	PPP	CCR
L+24	-0.55	21.93 (98/0/2)	15.55 (89/8/3)	27.93	34.60
L+23	-0.57	3.15 (0/100/0)	16.40 (87/11/3)	17.67	62.78
L+22	-0.57	26.93 (95/0/5)	29.42 (90/8/2)	19.72	23.93
L+8	-1.16	13.17 (0/100/0)	9.34 (86/10/4)	23.34	54.15
L+2	-1.50	15.55 (0/100/0)	11.39 (66/16/18)	69.52	3.53
L+1	-1.51	15.72 (25/0/75)	4.96 (40/42/18)	77.85	1.48
LUMO	-2.34	17.51 (0/100/0)	9.37 (28/49/23)	62.19	10.94
HOMO	-5.53	5.22 (20/0/80)	1.15 (59/27/13)	1.32	92.31
H-1	-5.63	0.11 (0/100/0)	0.65 (23/19/58)	3.75	95.50
H-4	-7.03	38.14 (12/0/88)	10.55 (13/17/69)	10.37	40.94

States	E, nm (eV)	O.S.	Transition (Contrib.)	Assignment	Exp. (nm)
S1	482 (2.57)	0.0853	HOMO→LUMO (96%)	^{1}LLCT/^{1}LMCT/^{1}IL	468
S4	353 (3.51)	0.5106	HOMO→L+2 (81%)	^{1}LLCT/^{1}LMCT	
S9	338 (3.67)	1.0933	H-1→L+1 (31%)	^{1}LLCT/^{1}LMCT	
			HOMO→L+8 (27%)	^{1}IL/^{1}LLCT/^{1}LMCT	
			H-4→LUMO (13%)	^{1}LLCT/^{1}MC/^{1}MLCT/^{1}IL	
S33	300 (4.14)	0.2968	HOMO→L+23 (42%)	^{1}IL/^{1}LLCT/^{1}LMCT	
			H-1→L+22 (21%)	^{1}LMCT/^{1}IL/^{1}LLCT	
			H-1→L+24 (14%)	^{1}LMCT/^{1}IL/^{1}LLCT	

Table S6. The Partial Molecular Orbital Compositions (%) by SCPA Approach in the Lowest-Energy Triplet State and the Emission Transition for Complex **2** in the CH_2Cl_2 Solution Calculated by TD-DFT Method at the PBE1PBE Level.

Orbital	Energy (eV)	MO Contribution (%)			
		Pt (s/p/d)	Ag (s/p/d)	PPP	CCR
L+11	-1.07	11.40 (46/0/54)	10.52 (55/30/14)	22.93	55.14
L+8	-1.26	4.70 (0/100/0)	2.08 (42/51/7)	29.40	63.82
LUMO	-2.75	21.46 (0/100/0)	24.98 (80/8/12)	47.13	6.43
HOMO	-5.45	4.84 (23/0/77)	1.54 (67/20/13)	1.91	91.70
H-1	-5.56	0.71 (0/100/0)	1.57 (83/8/9)	3.57	94.16

States	E, nm (eV)	O.S.	Transition (Contrib.)	Assignment	Exp. (nm)
T1	605 (2.05)	0.0000	HOMO→LUMO (92%)	^{3}LLCT/^{3}LMCT	636
T2	558 (2.22)	0.0000	H-1→LUMO (91%)	^{3}LLCT/^{3}LMCT	
T3	485 (2.56)	0.0000	HOMO→L+8 (42%)	^{3}IL/^{3}LLCT	
			H-1→L+11 (25%)	^{3}IL/^{3}LLCT/^{3}LMCT	

Table S7. The Partial Molecular Orbital Compositions (%) by SCPA Approach in the Ground State and the Absorption Transition for Complex **3** in the CH_2Cl_2 Solution Calculated by TD-DFT Method at the PBE1PBE Level.

Orbital	Energy (eV)	MO Contribution (%)			
		Pt (s/p/d)	Ag (s/p/d)	PPP	CCR
L+5	-1.61	6.87 (0/100/0)	11.38 (28/62/11)	45.24	36.51
L+2	-2.03	7.66 (0/100/0)	7.41 (55/37/8)	36.52	48.41
L+1	-2.26	19.35 (86/0/14)	16.97 (83/15/2)	4.53	59.15
LUMO	-2.79	13.44 (0/100/0)	13.02 (65/20/15)	39.06	34.48
HOMO	-6.49	20.49 (20/0/80)	7.00 (57/10/34)	6.83	65.69
H-1	-6.84	1.63 (0/100/0)	17.03 (42/8/50)	20.51	60.84
H-2	-6.89	28.14 (36/0/64)	34.64 (39/12/49)	35.38	1.85

States	E, nm (eV)	O.S.	Transition (Contrib.)	Assignment	Exp. (nm)
S1	416 (2.98)	1.0329	HOMO→LUMO (95%)	^{1}IL/^{1}LLCT/^{1}MC	410
S2	371 (3.35)	0.5130	H-2→LUMO (94%)	^{1}IL/^{1}MLCT/^{1}MC	370
S6	328 (3.78)	0.3746	HOMO→L+2 (77%)	^{1}IL/^{1}LLCT/^{1}MLCT/^{1}MC	319
			H-1→L+1 (17%)	^{1}IL/^{1}LMCT/^{1}MC	
S14	299 (4.15)	0.4101	HOMO→L+5 (62%)	^{1}IL/^{1}LLCT/^{1}MC/^{1}MLCT	

Table S8. The Partial Molecular Orbital Compositions (%) by SCPA Approach in the Lowest-Energy Triplet State and the Emission Transition for Complex **3** in the CH_2Cl_2 Solution Calculated by TD-DFT Method at the PBE1PBE Level.

Orbital	Energy (eV)	MO Contribution (%)			
		Pt (s/p/d)	Ag (s/p/d)	PPP	CCR
L+2	-2.07	9.28 (9/89/2)	7.78 (56/37/7)	36.39	46.55
L+1	-2.37	17.75 (77/9/15)	15.39 (80/17/3)	10.08	56.78
LUMO	-3.00	14.06 (4/95/1)	12.89 (68/16/16)	32.99	40.06
HOMO	-6.27	18.54 (23/1/76)	5.94 (57/12/31)	5.16	70.36
H-1	-6.76	3.92 (12/38/50)	15.01 (42/8/49)	18.22	62.85

States	E, nm (eV)	O.S.	Transition (Contrib.)	Assignment	Exp. (nm)
T1	598 (2.07)	0.0000	HOMO→LUMO (70%)	^{3}IL/^{3}LLCT/^{3}MC	534
			HOMO→L+1 (13%)	^{3}IL/^{3}MC/^{3}LMCT	
T2	533 (2.33)	0.0000	H-1→LUMO (31%)	^{3}IL/^{3}MC/^{3}LLCT	
			HOMO→L+1 (22%)	^{3}IL/^{3}MC/^{3}LMCT	
			H-1→L+1 (14%)	^{3}IL/^{3}MC/^{3}LMCT	
T3	435 (2.85)	0.0000	HOMO→L+2 (26%)	^{3}IL/^{3}LLCT/^{3}MC	
			H-1→L+1 (14%)	^{3}IL/^{3}MC/^{3}LMCT	
			HOMO→LUMO (13%)	^{3}IL/^{3}LLCT/^{3}MC	
			HOMO→L+1 (12%)	^{3}IL/^{3}MC/^{3}LMCT	

Table S9. The Partial Molecular Orbital Compositions (%) by SCPA Approach in the Ground State and the Absorption Transition for Complex **4** in the CH_2Cl_2 Solution Calculated by TD-DFT Method at the PBE1PBE Level.

Orbital	Energy (eV)	MO Contribution (%)			
		Pt (s/p/d)	Ag (s/p/d)	PPP	CCR
L+2	-1.9	6.72 (0/100/0)	5.76 (38/55/7)	42.05	45.47
L+1	-2.13	32.60 (95/0/5)	22.48 (80/19/2)	3.60	41.32
LUMO	-2.77	13.00 (0/100/0)	11.60 (58/25/17)	43.29	32.11
HOMO	-6.37	15.58 (12/0/88)	4.71 (44/12/44)	4.99	74.73
H-1	-6.65	0.70 (0/100/0)	10.21 (35/9/56)	12.63	76.46
H-2	-6.87	25.53 (35/0/65)	35.36 (40/11/49)	36.84	2.28

States	E, nm (eV)	O.S.	Transition (Contrib.)	Assignment	Exp. (nm)
S1	424 (2.92)	1.3958	HOMO→LUMO (94%)	^{1}LLCT/^{1}IL/^{1}MC	411
S3	370 (3.35)	0.5623	H-2→LUMO (94%)	^{1}IL/^{1}MLCT/^{1}MC	370
S6	325 (3.82)	1.6354	HOMO→L+2 (66%)	^{1}IL/^{1}LLCT/^{1}MC	317
			H-1→L+1 (25%)	^{1}LMCT/^{1}IL/^{1}MC	

Table S10. The Partial Molecular Orbital Compositions (%) by SCPA Approach in the Lowest-Energy Triplet State and the Emission Transition for Complex **4** in the CH_2Cl_2 Solution Calculated by TD-DFT Method at the PBE1PBE Level.

Orbital	Energy (eV)	MO Contribution (%)			
		Pt (s/p/d)	Ag (s/p/d)	PPP	CCR
L+2	-1.97	10.05 (31/67/2)	7.52 (50/43/7)	37.91	44.52
L+1	-2.28	29.38 (90/4/6)	20.28 (78/19/2)	8.46	41.88
LUMO	-2.96	14.37 (6/93/1)	12.08 (64/19/17)	37.24	36.31
HOMO	-6.13	12.22 (14/1/85)	3.61 (44/13/43)	3.99	80.17
H-1	-6.58	3.35 (7/17/75)	8.21 (35/9/55)	10.53	77.91
H-3	-7.21	18.83 (35/3/62)	8.62 (43/16/42)	14.85	57.71

States	E, nm (eV)	O.S.	Transition (Contrib.)	Assignment	Exp. (nm)
T1	601 (2.06)	0.0000	HOMO→LUMO (68%)	^{3}IL/^{3}LLCT/^{3}MC/^{3}LMCT	522
			HOMO→L+1 (18%)	^{3}IL/^{3}LMCT/^{3}MC	
T2	537 (2.31)	0.0000	H-1→LUMO (38%)	^{3}IL/^{3}LLCT/^{3}LMCT/^{3}MC	
			HOMO→L+1 (18%)	^{3}IL/^{3}LMCT/^{3}MC	
			H-1→L+1 (13%)	^{3}IL/^{3}LMCT/^{3}MC	
			H-1→L+2 (10%)	^{3}IL/^{3}LLCT/^{3}MC	
T3	459 (2.70)	0.0000	H-3→LUMO (15%)	^{3}IL/^{3}MC/^{3}LLCT	
			HOMO→L+2 (14%)	^{3}IL/^{3}LLCT/^{3}MC	
			H-1→L+1 (13%)	^{3}IL/^{3}LMCT/^{3}MC	
			HOMO→L+1 (10%)	^{3}IL/^{3}LMCT/^{3}MC	

Table S11. The Partial Molecular Orbital Compositions (%) by SCPA Approach in the Ground State and the Absorption Transition for Complex **5** in the CH_2Cl_2 Solution Calculated by TD-DFT Method at the PBE1PBE Level.

Orbital	Energy (eV)	MO Contribution (%)			
		Pt (s/p/d)	Ag (s/p/d)	PPP	CCR
L+4	-2.03	8.03 (0/100/0)	5.22 (28/60/12)	43.37	43.38
L+3	-2.19	0.32 (9/88/3)	0.45 (87/9/4)	0.14	99.08
L+2	-2.19	0.29 (65/15/20)	0.32 (80/7/13)	0.20	99.19
L+1	-2.29	28.31 (94/0/6)	19.13 (80/19/2)	2.53	50.03
LUMO	-2.78	12.14 (0/100/0)	11.03 (60/23/16)	39.00	37.83
HOMO	-6.47	21.13 (16/0/84)	7.70 (47/10/43)	8.32	62.84
H-1	-6.84	1.76 (0/100/0)	21.58 (38/7/55)	26.30	50.35
H-2	-6.86	28.54 (34/0/66)	34.34 (38/12/50)	34.88	2.24
H-4	-7.38	0.12 (0/100/0)	0.09 (40/41/18)	2.04	97.75
H-5	-7.38	0.06 (43/0/56)	0.21 (75/15/10)	0.73	99.00
H-8	-7.44	0.35 (0/100/0)	2.15 (62/2/36)	4.02	93.49
H-9	-7.44	0.81 (22/0/78)	0.48 (15/53/32)	4.74	93.96
H-17	-7.61	0.97 (86/0/14)	0.82 (72/25/4)	1.30	96.92
H-25	-7.83	5.51 (48/0/52)	2.30 (24/7/69)	89.97	2.22

States	E, nm (eV)	O.S.	Transition (Contrib.)	Assignment	Exp. (nm)
S1	417 (2.97)	1.2582	HOMO→LUMO (95%)	^{1}IL/^{1}LLCT/^{1}MC	412
S2	371 (3.34)	0.5637	H-2→LUMO (93%)	^{1}MLCT/^{1}IL/^{1}MC	371
S8	325 (3.82)	0.9648	HOMO→L+4 (80%)	^{1}IL/^{1}LLCT/^{1}MLCT/^{1}MC	330
			H-1→L+1 (13%)	^{1}IL/^{1}LMCT/^{1}MC	
S55	278 (4.46)	0.5505	H-25→LUMO (20%)	^{1}IL/^{1}LLCT/^{1}LMCT	
			H-8→L+2 (20%)	^{1}IL	
			H-9→L+3 (19%)	^{1}IL	
S65	271 (4.57)	0.5916	H-4→L+1 (32%)	^{1}IL/^{1}LMCT	269
			H-17→L+3 (14%)	^{1}IL	
			H-5→LUMO (13%)	^{1}LLCT/^{1}IL/^{1}LMCT	
			H-5→L+4 (11%)	^{1}IL/^{1}LLCT	

Table S12. The Partial Molecular Orbital Compositions (%) by SCPA Approach in the Lowest-Energy Triplet State and the Emission Transition for Complex **5** in the CH_2Cl_2 Solution Calculated by TD-DFT Method at the PBE1PBE Level.

Orbital	Energy (eV)	MO Contribution (%)			
		Pt (s/p/d)	Ag (s/p/d)	PPP	CCR
L+1	-2.29	26.62 (93/0/7)	17.74 (80/19/1)	2.48	53.15
LUMO	-2.95	16.30 (0/100/0)	15.01 (71/13/15)	39.34	29.35
HOMO	-6.31	24.80 (23/0/77)	4.60 (63/9/28)	3.66	66.94
H-1	-6.8	2.54 (0/100/0)	17.01 (38/7/55)	21.83	58.62
H-2	-6.9	26.31 (40/0/60)	35.76 (39/12/49)	37.05	0.88

States	*E*, nm (eV)	O.S.	Transition (Contrib.)	Assignment	Exp. (nm)
T1	584 (2.12)	0.0000	HOMO→LUMO (81%)	^{3}LLCT/^{3}IL/^{3}MC	517
T2	523 (2.37)	0.0000	H-1→LUMO (44%) HOMO→L+1 (32%)	^{3}IL/^{3}LLCT/^{3}MC/^{3}LMCT ^{3}IL/^{3}MC/^{3}LMCT	
T3	428 (2.90)	0.0000	H-2→LUMO (85%)	^{3}IL/^{3}MC/^{3}MLCT	

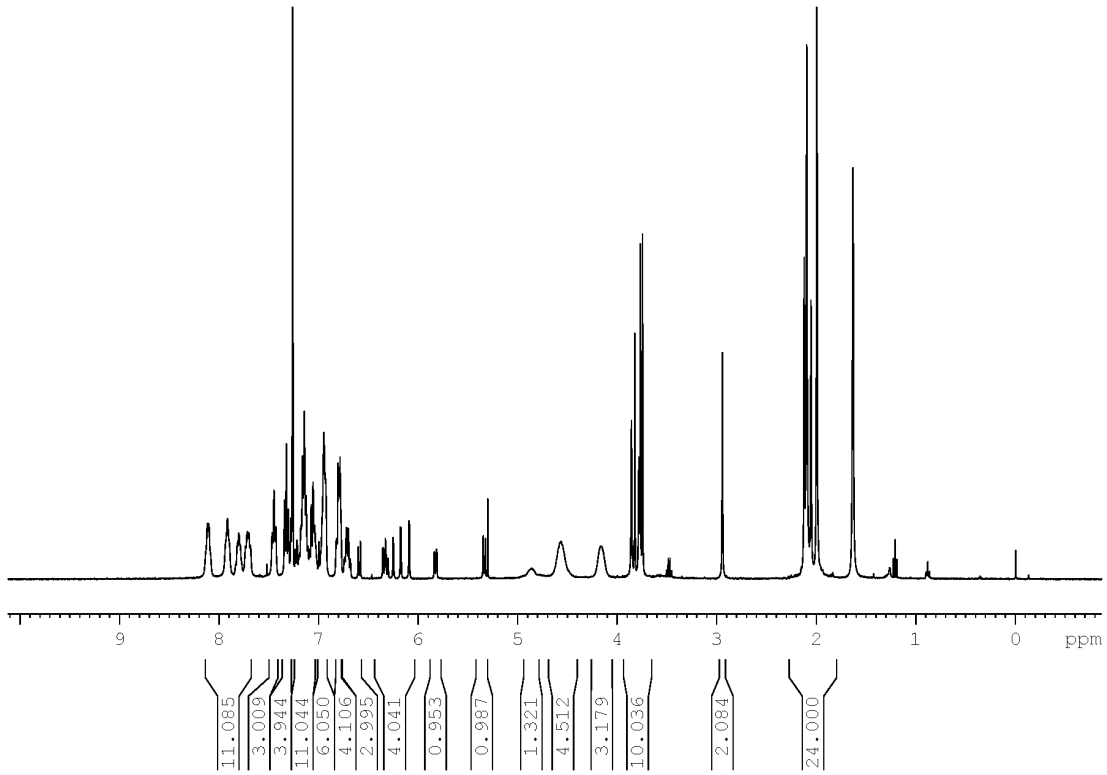

Fig. S1 The ^{1}H NMR spectrum of complex **1** in $CDCl_3$ solution at ambient temperature.

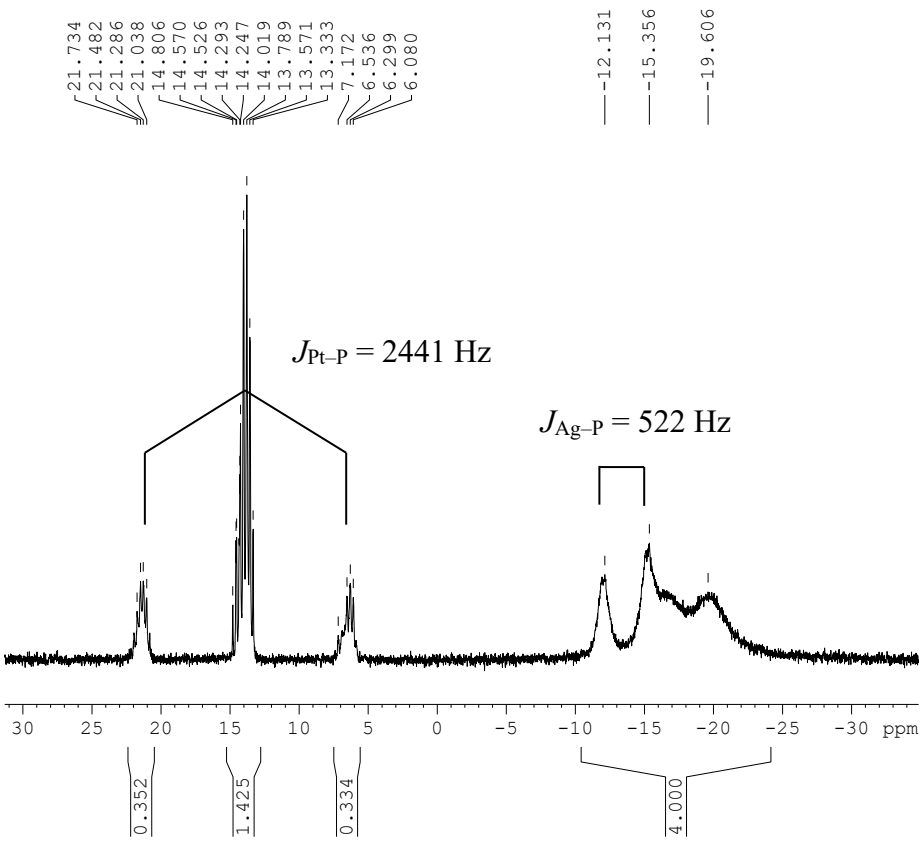

Fig. S2 The ^{31}P NMR spectrum of complex **1** in $CDCl_3$ solution at ambient temperature.

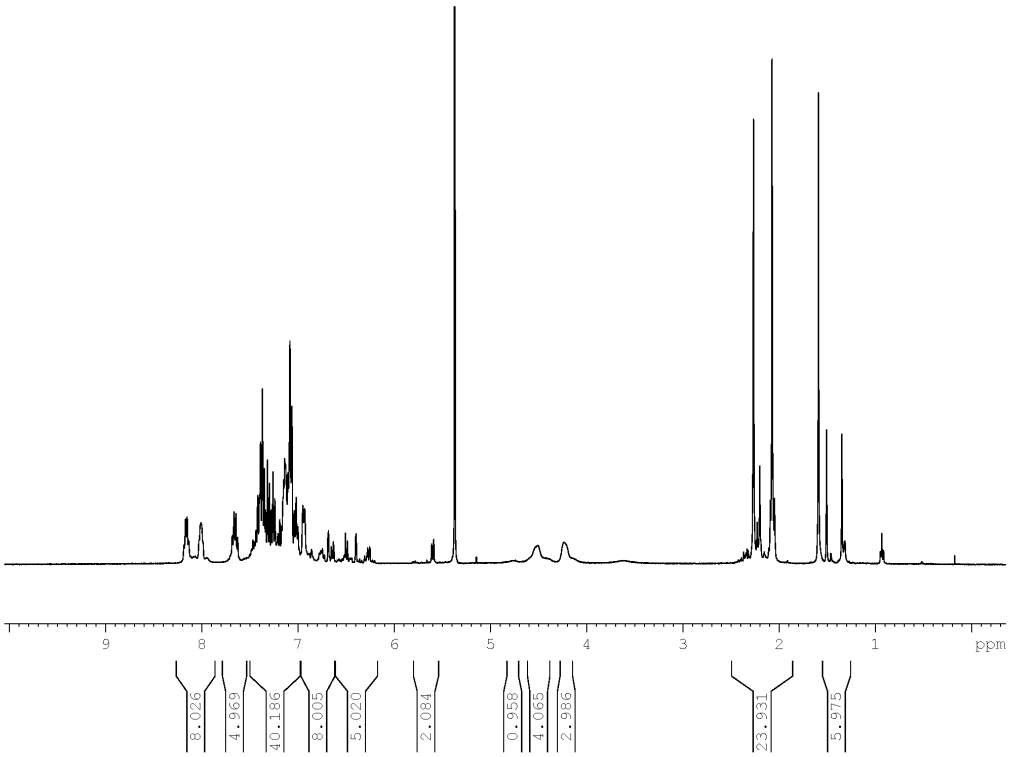

Fig. S3 The ^{1}H NMR spectrum of complex **2** in CD_2Cl_2 solution at ambient temperature.

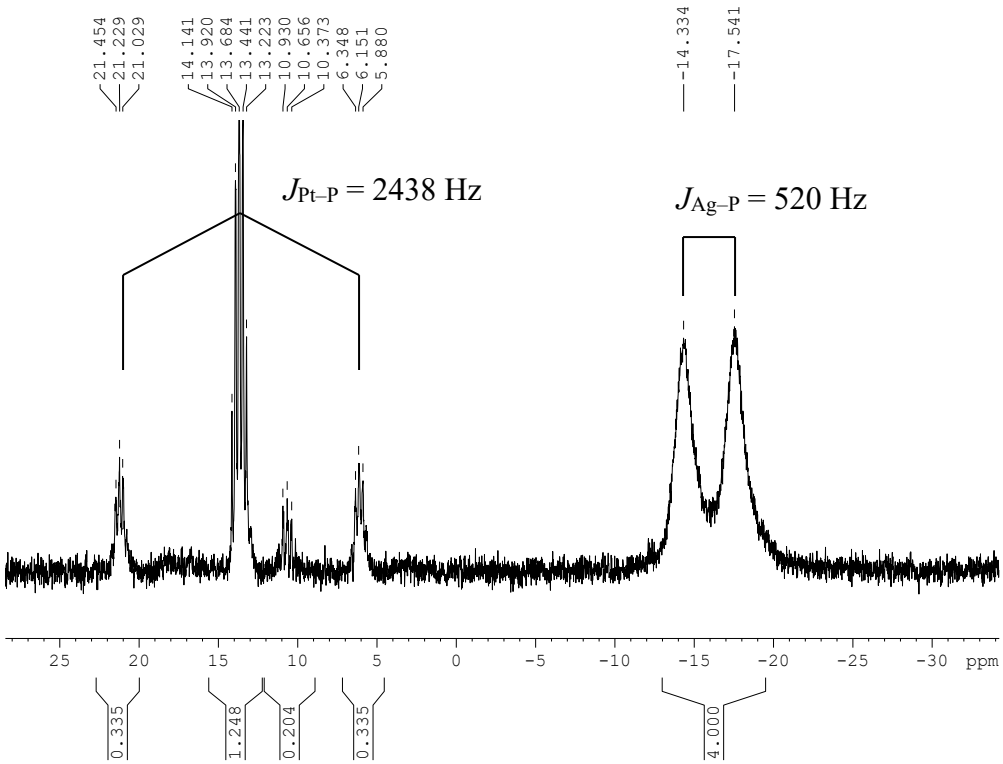

Fig. S4 The ^{31}P NMR spectrum of complex **2** in CD_2Cl_2 solution at ambient temperature.

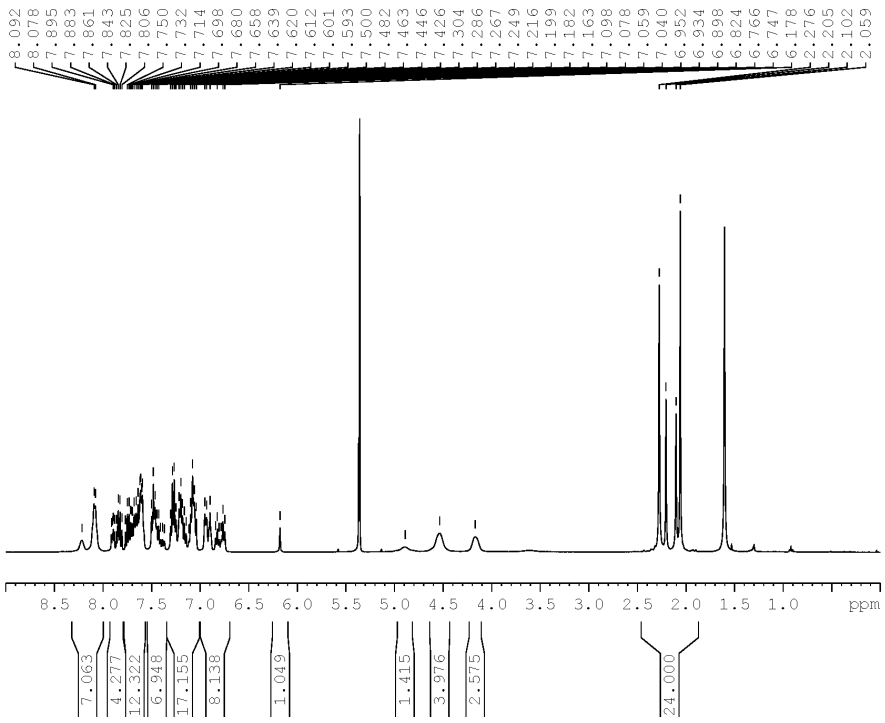

Fig. S5 The ^{1}H NMR spectrum of complex **3** in CD_2Cl_2 solution at ambient temperature.

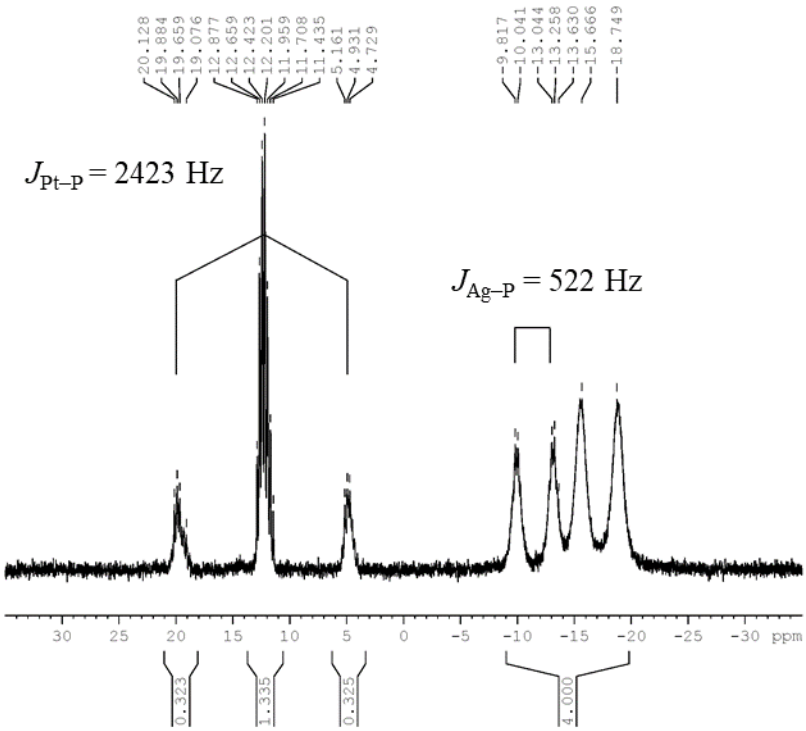

Fig. S6 The ^{31}P NMR spectrum of complex **3** in CD_2Cl_2 solution at ambient temperature.

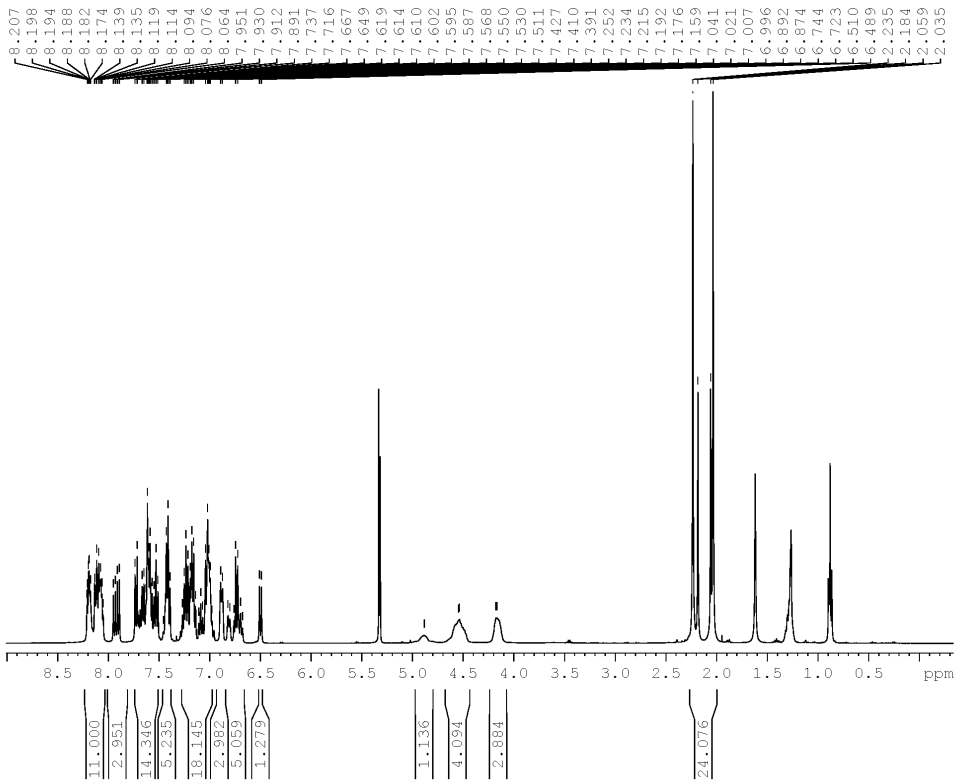

Fig. S7 The ^{1}H NMR spectrum of complex **4** in CD_2Cl_2 solution at ambient temperature.

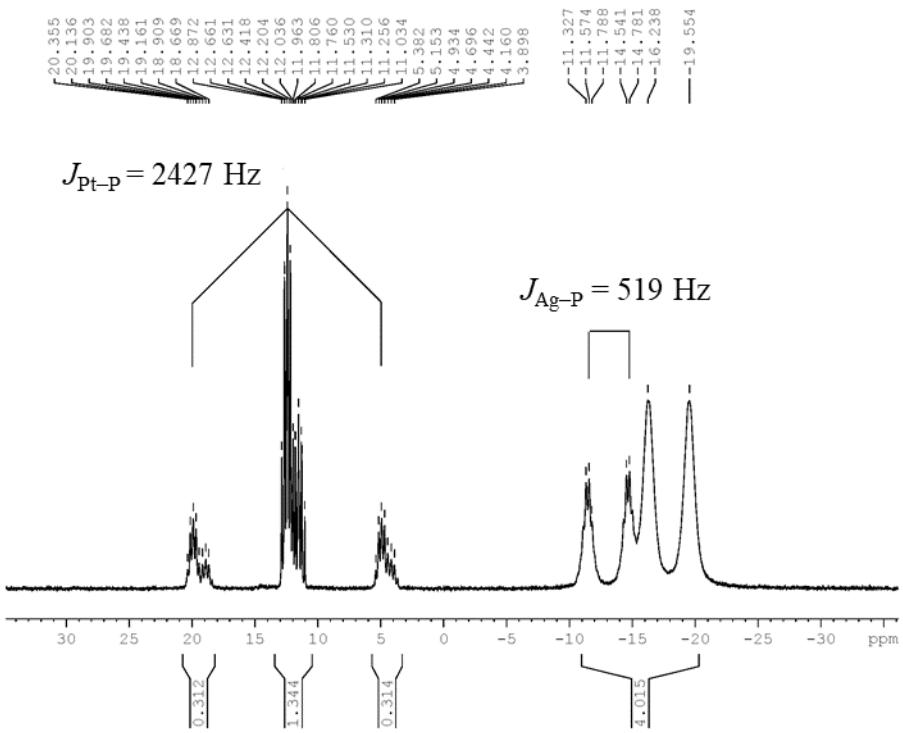

Fig. S8 The ^{31}P NMR spectrum of complex **4** in CD_2Cl_2 solution at ambient temperature.

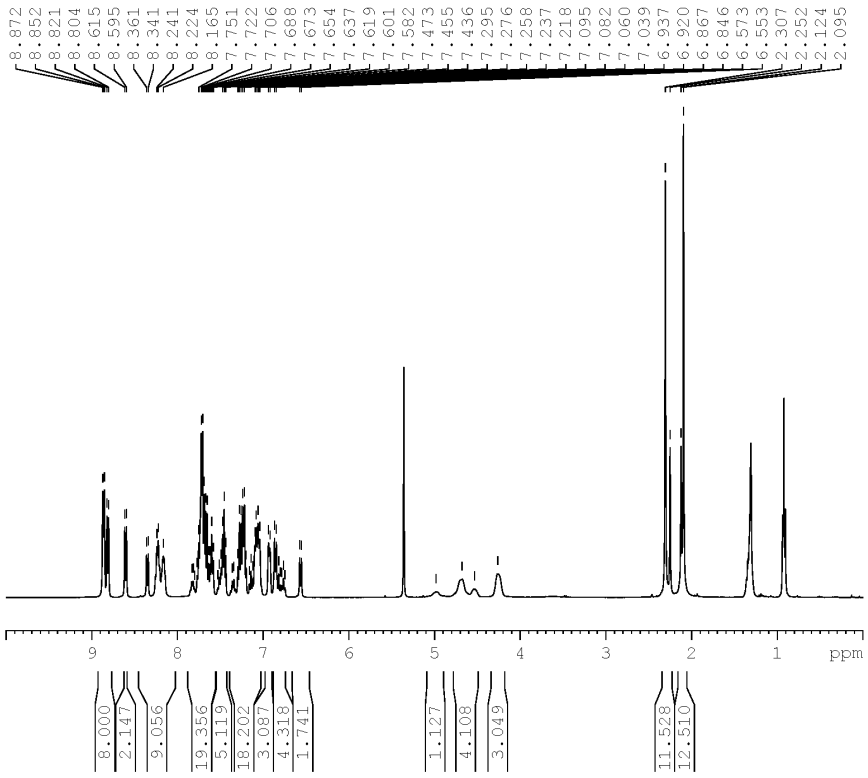

Fig. S9 The ^{1}H NMR spectrum of complex **5** in CD_2Cl_2 solution at ambient temperature.

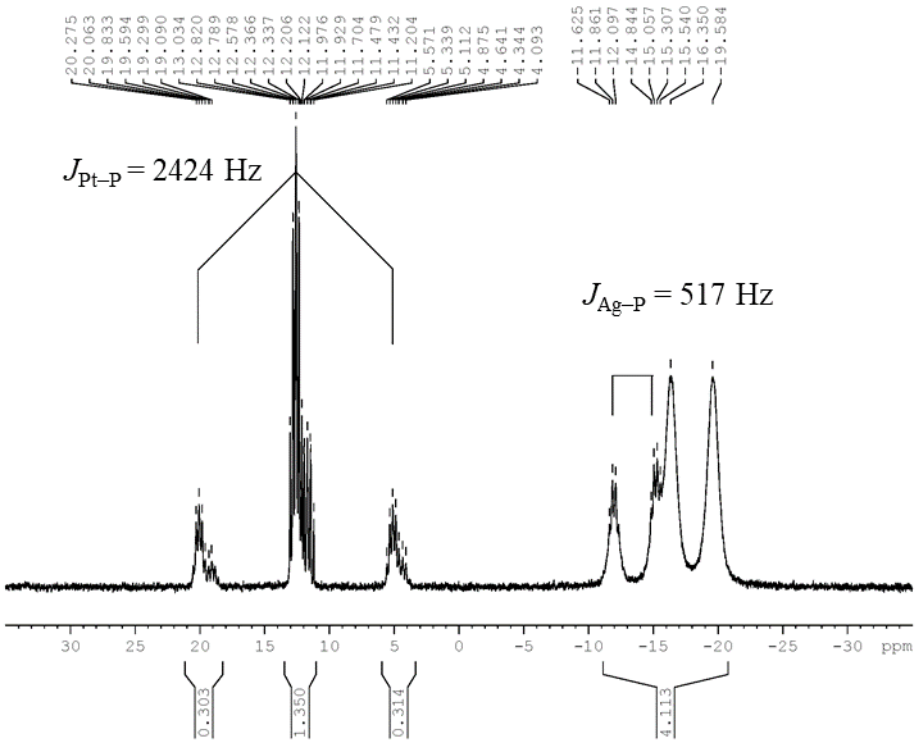

Fig. S10 The ^{31}P NMR spectrum of complex **5** in CD_2Cl_2 solution at ambient temperature.

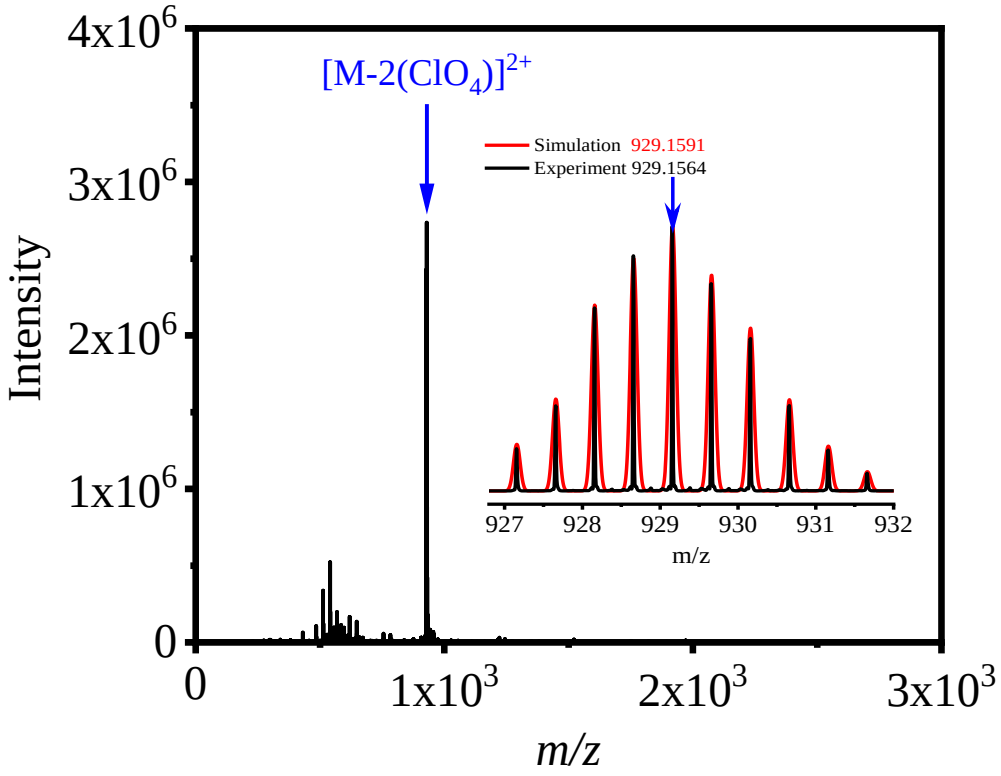

Fig. S11 The high-resolution mass spectrometry of $PtAg_2$ complex **1**. Inset: The measured and simulated isotopic patterns.

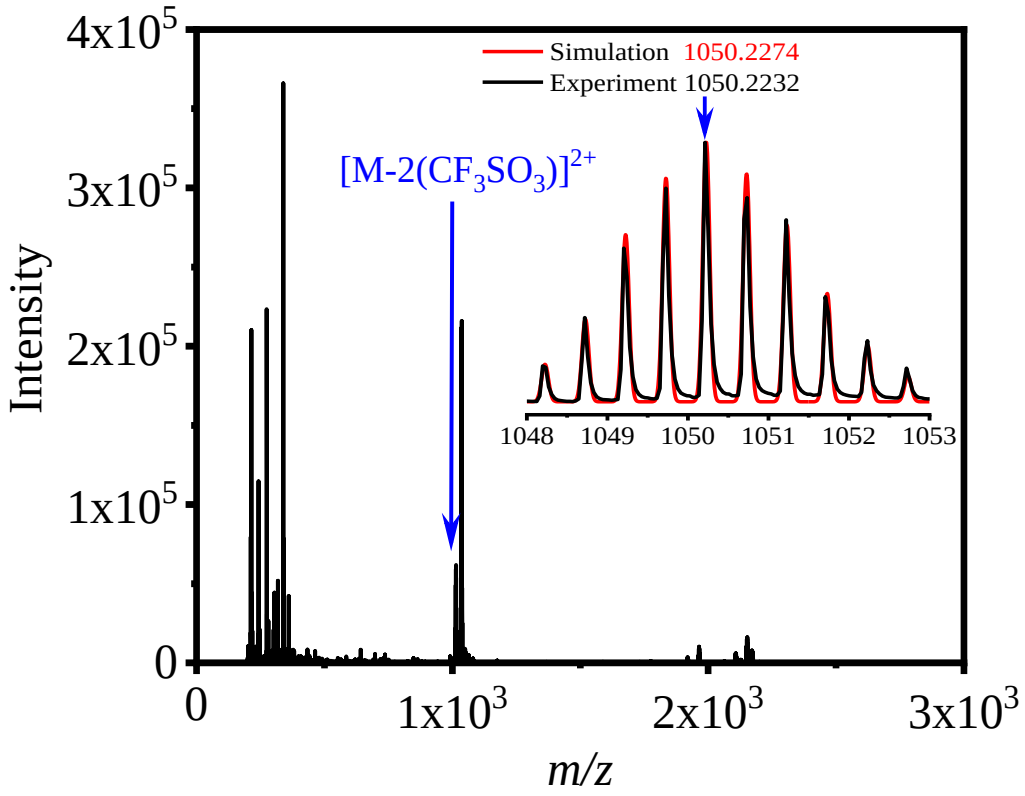

Fig. S12 The high-resolution mass spectrometry of $PtAg_2$ complex **2**. Inset: The measured and simulated isotopic patterns.

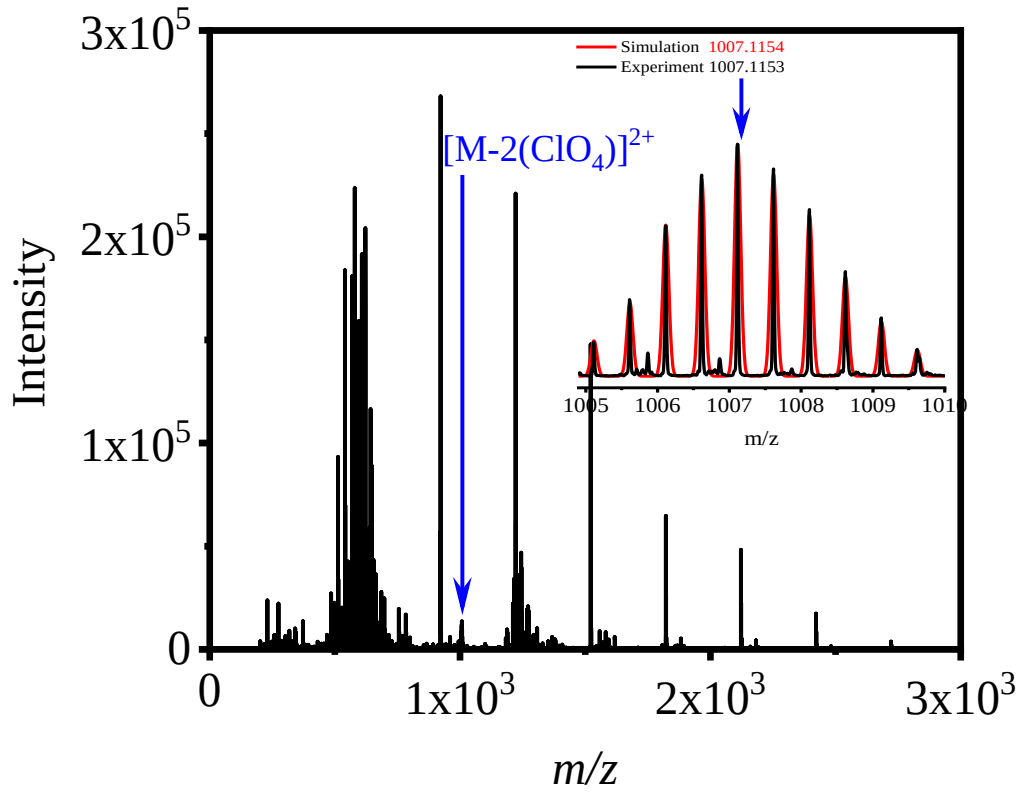

Fig. S13 The high-resolution mass spectrometry of $PtAg_2$ complex **3**. Inset: The measured and simulated isotopic patterns.

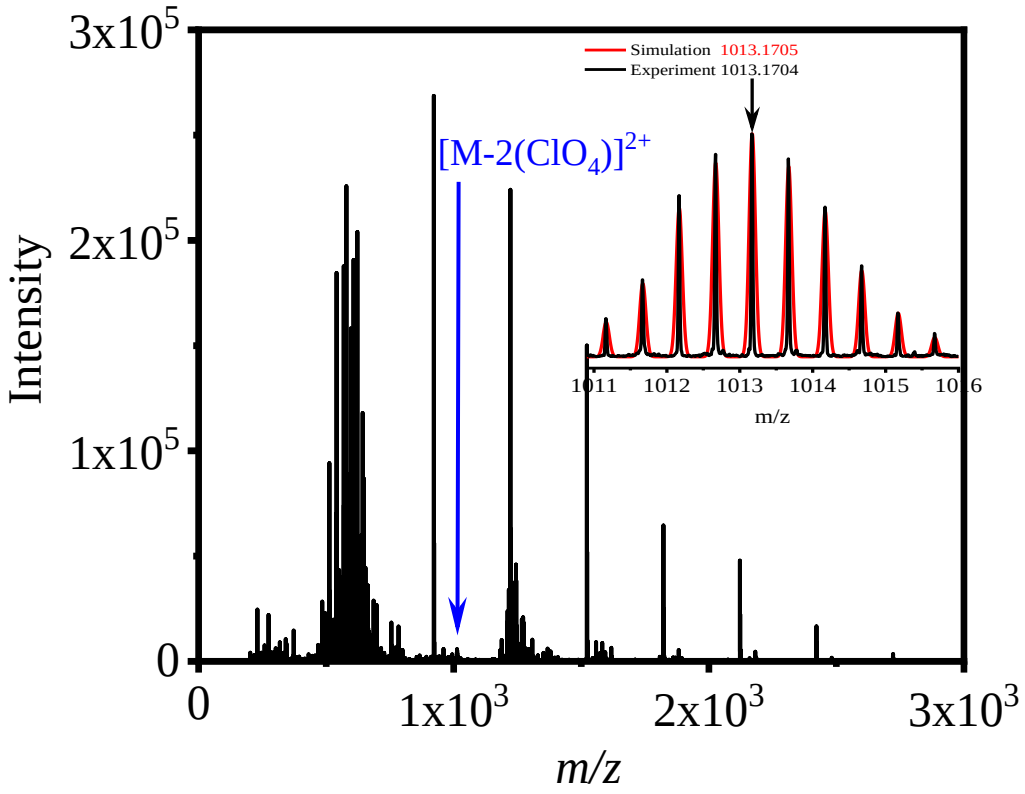

Fig. S14 The high-resolution mass spectrometry of $PtAg_2$ complex **4**. Inset: The measured and simulated isotopic patterns.

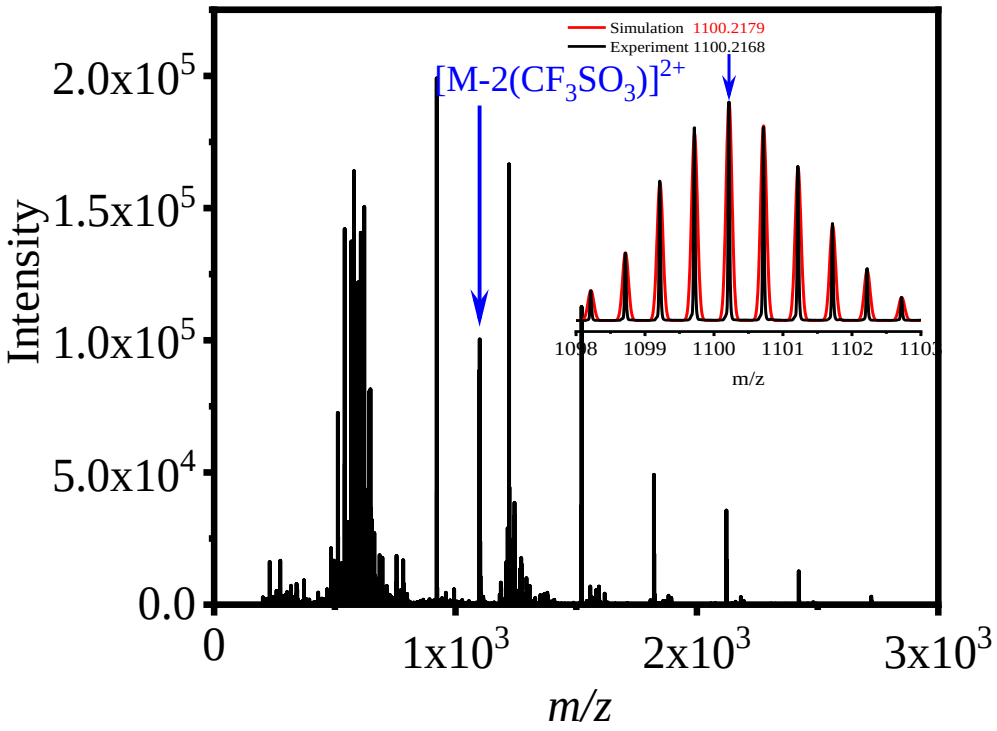

Fig. S15 The high-resolution mass spectrometry of $PtAg_2$ complex **5**. Inset: The measured and simulated isotopic patterns.

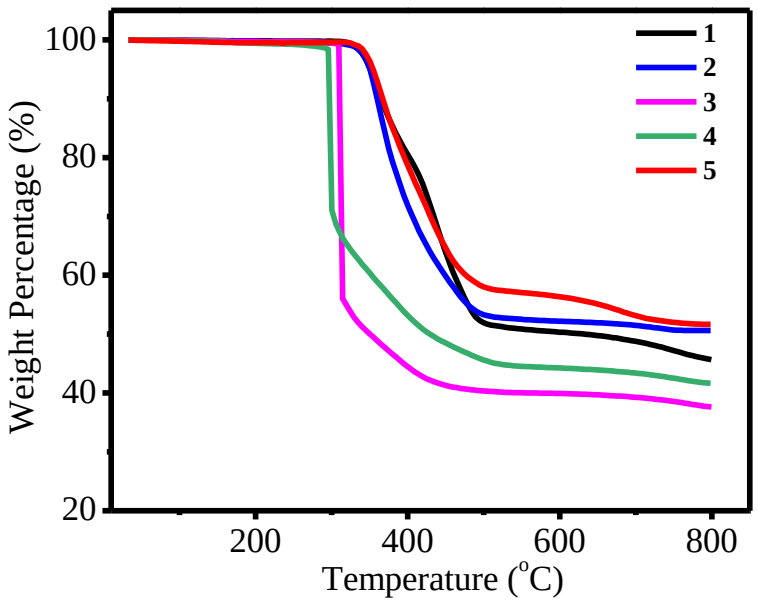

Fig. S16 Thermogravimetric analysis for complexes **1-5.**

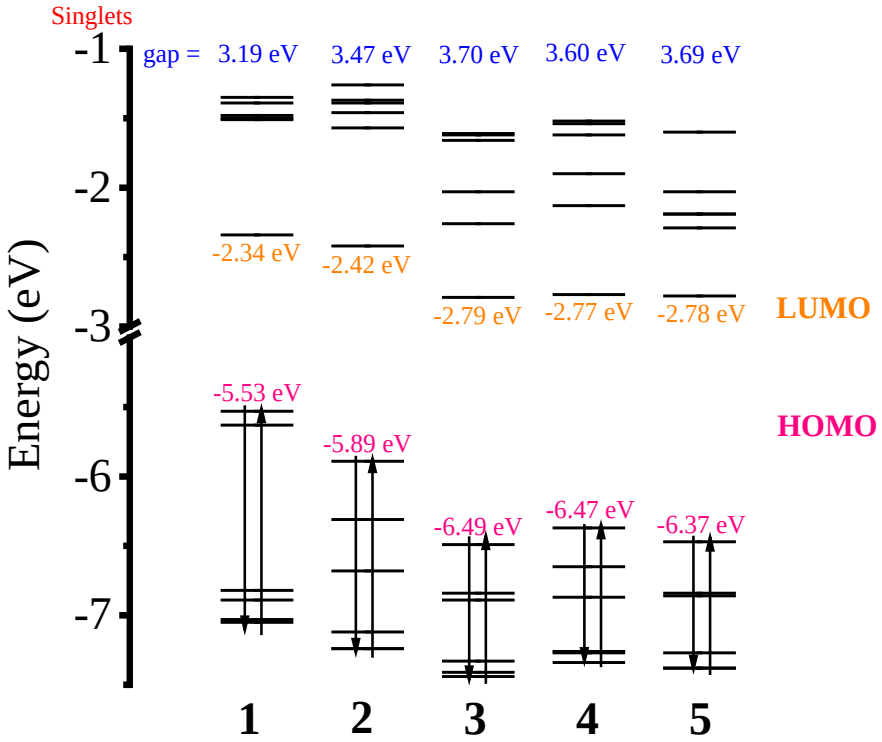

Fig. S17 Plots of energy level of frontier orbitals in the ground states for complexes **1-5**, respectively, in the CH_2Cl_2 solution by TD-DFT method at the PBE1PBE level.

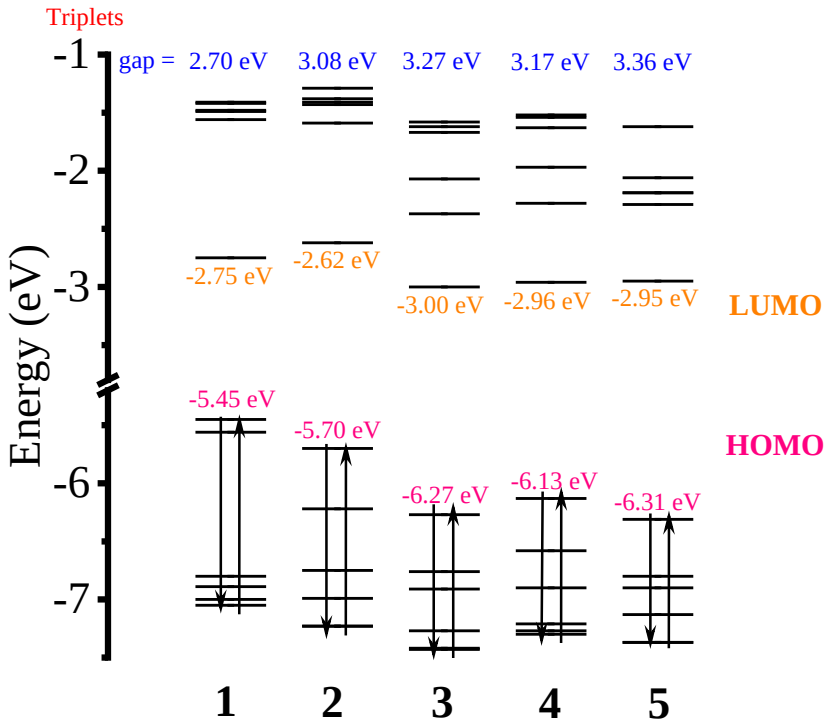

Fig. S18 Plots of energy level of frontier orbitals in the lowest-energy triplet states for complexes **1-5**, respectively, in the CH_2Cl_2 solution by TD-DFT method at the PBE1PBE level.

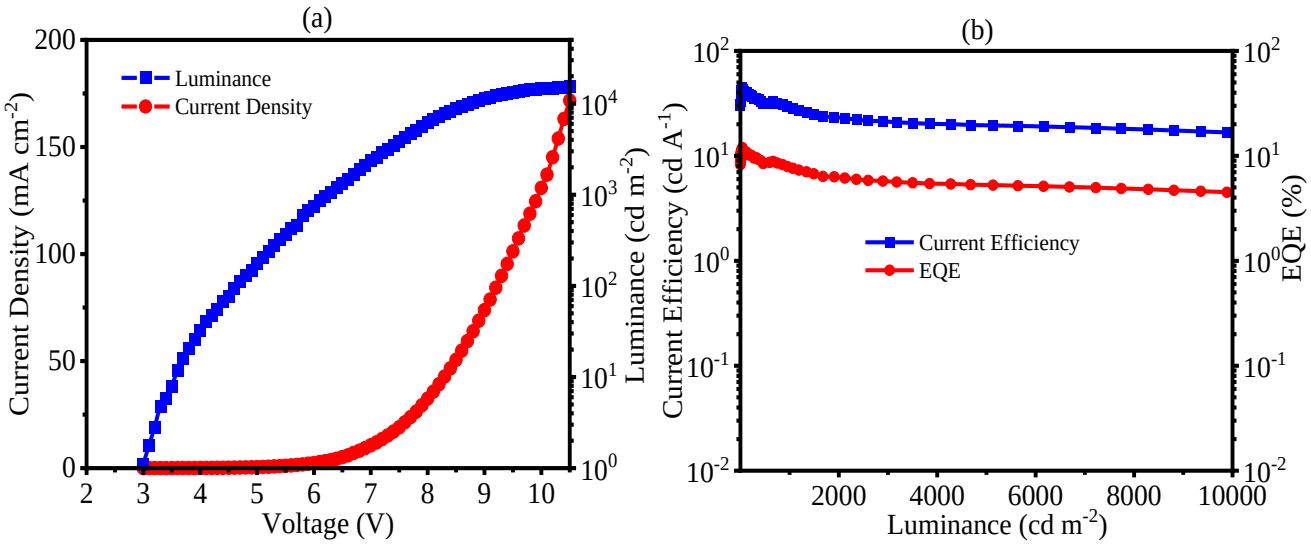

Fig. S19 (a) Current density-voltage-luminance characteristics. (b) Current efficiency/external quantum efficiency *vs* luminance for OLED based on complex **1**.

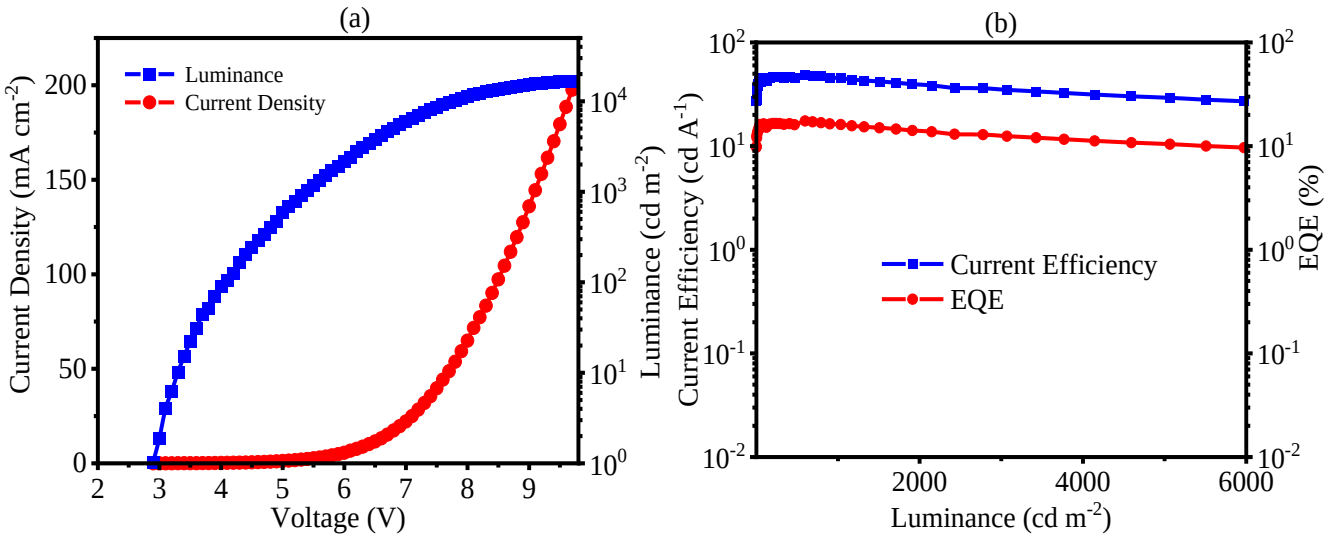

Fig. S20 (a) Current density-voltage-luminance characteristics. (b) Current efficiency/external quantum efficiency *vs* luminance for OLED based on complex **2**.

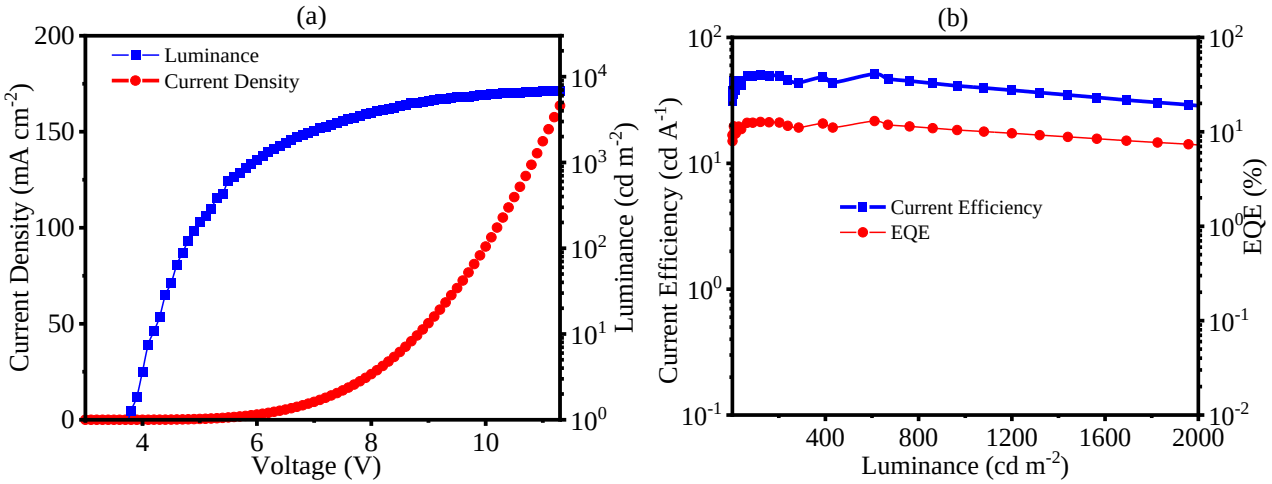

Fig. S21 (a) Current density-voltage-luminance characteristics. (b) Current efficiency/external quantum efficiency *vs* luminance for OLED based on complex **3**.

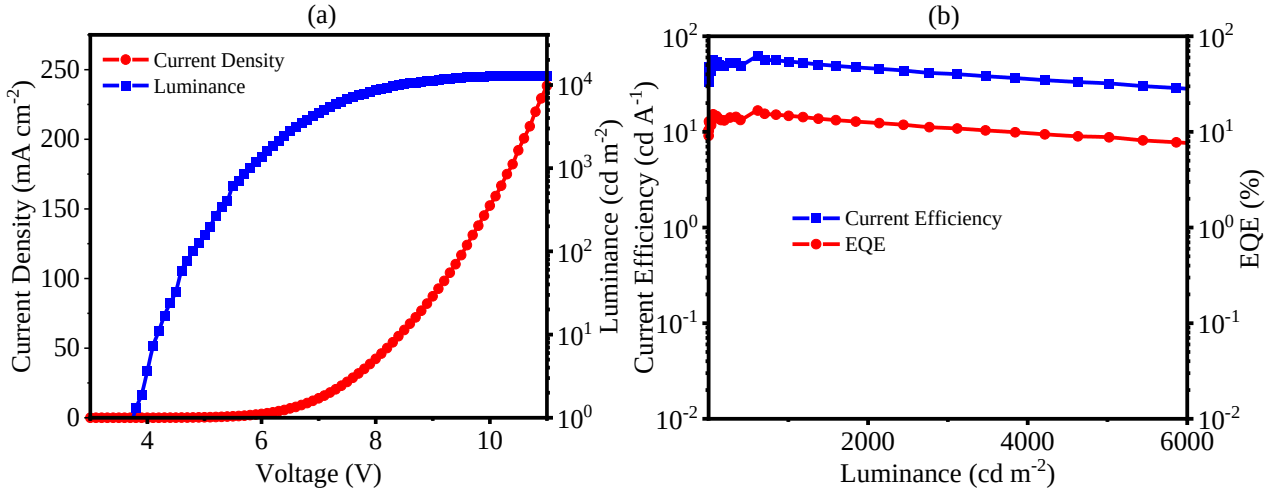

Fig. S22 (a) Current density-voltage-luminance characteristics. (b) Current efficiency/external quantum efficiency *vs* luminance for OLED based on complex **5**.